*universe*

MDPI

*Review*

# Strange Dwarfs: A Review on the (in)Stability

**Francesco Di Clemente [1], Alessandro Drago [1,2,*] and Giuseppe Pagliara [1,2]**

[1] Istituto Nazionale di Fisica Nucleare, Sezione di Ferrara, via Saragat 1, I-44122 Ferrara, Italy; fdiclemente@fe.infn.it (F.D.C.); pagliara@fe.infn.it (G.P.)
[2] Department of Physics and Earth Science, University of Ferrara, via Saragat 1, I-44122 Ferrara, Italy
* Correspondence: drago@fe.infn.it

**Abstract:** White dwarfs are the remnants of stars not massive enough to become supernovae. This review explores the concept of strange dwarfs, a unique class of white dwarfs that contain cores of strange quark matter. Strange dwarfs have different sizes, masses, and evolutionary paths with respect to white dwarfs. They might form through the accumulation of normal matter on strange quark stars or by the capture of strangelets. The stability of strange dwarfs has been debated, with initial studies suggesting stability, while later analyses indicated potential instability. This review revisits these discussions, focusing on the critical role of boundary conditions between nuclear and quark matter in determining stability. It also offers insights into their formation, structure, and possible detection in the universe.

**Keywords:** strange matter; white dwarfs; accretion-induced collapse



**Citation:** Di Clemente, F.; Drago, A.; Pagliara, G. Strange Dwarfs: A Review on the (in)Stability. *Universe* **2024**, *10*, 322. https://doi.org/10.3390/universe10080322

Academic Editors: Ana Gabriela Grunfeld and David Blaschke

Received: 5 June 2024
Revised: 6 August 2024
Accepted: 7 August 2024
Published: 9 August 2024



## 1. Introduction

White dwarfs (WDs) are astrophysical objects that originate from the remnants of stars whose initial mass was below approximately 9 $M_\odot$ [1]. These stars, after depleting their reserves of nuclear fuel, enter a phase during which their cores contract because nuclear reactions can no longer counteract gravitational forces, while their outer layers expand. This collapse is halted only when the electrons within the star core become degenerate, providing the necessary pressure to counteract further gravitational collapse. Depending on the mass of the progenitor, the stellar outcome can be different. Indeed, the nuclear fusion reactions that occur during the star's evolution can result in the formation of different nuclei, ultimately influencing the nature of the resulting WDs, such as helium (He), carbon–oxygen (C-O), and oxygen–neon–magnesium (O-Ne-Mg) WDs. It is essential to note that the maximum mass that a WD can attain, referred to as the Chandrasekhar mass and calculated to be approximately 1.4 $M_\odot$ [2], varies depending on the composition of the WD. In practice, the majority of observed WDs are of the C-O type.

In work by Glendenning et al. [3,4], it was proposed that WDs could possess an inner core composed of absolutely stable strange quark matter. This is a consequence of the Bodmer–Witten hypothesis [5,6]. What makes this idea even more interesting is that the presence of this stable strange quark matter core has the potential to make some of these compact objects stable, while the corresponding configuration without the strange quark core would be unstable.

These objects, named "strange dwarfs" (SDs), exhibit characteristics distinct from those of conventional WDs. Specifically, they can have different radii, masses, and astrophysical evolution. It was conjectured that SDs could form either by accumulating normal nuclear matter on the surface of a strange quark star (SQS) or by collecting clusters of strange quark matter, commonly referred to as "strangelets", onto WDs.

Glendenning et al. [3] studied the radial oscillations of SDs to assess their stability, finding that they can remain stable even if the density of the nuclear matter envelope surpasses the maximum density observed in typical WDs.

The question concerning the stability of SDs underwent a thorough reexamination in the work of Alford et al. [7]. By studying the fundamental radial mode, they found those objects to be unstable under radial oscillations.

It was suggested that the previous works by Glendenning et al. [3,4] may have inadvertently misinterpreted their findings by confusing the second–lowest eigenmode with the lowest one. However, upon closer examination and analysis, it became evident that these two research studies were built upon different underlying hypotheses [8]. Contrary to the initial belief that the two studies were grounded on the same assumptions, it became clear that they operated within slightly distinct theoretical frameworks, each with its own validity. This realization effectively solved the apparent contradiction between the results obtained by the two works. Specifically, Di Clemente et al. [8] and Di Clemente [9] focused on the boundary conditions between the nuclear matter and the quark core. The analysis is based on the formalism established in work by Pereira et al. [10] and Di Clemente et al. [11]. These studies provide insights into the boundary conditions that ought to be applied in the context of rapid (and slow) conversions between nuclear matter and quark matter and in the context of phase transitions in general. Crucially, the specific boundary conditions employed can exert a substantial influence on the eigenvalues governing radial oscillations, and, by extension, they can have a profound impact on the overall stability of the star. In addition, Di Clemente et al. [8] also addressed the applicability of the stability criterion based on the analysis of the extrema of the MR curve [12,13]. However, in this specific case, a crucial refinement is added to this criterion, by emphasizing the need for explicit specification regarding whether the quark content of the star remains constant or undergoes changes during the radial oscillations.

In this review, based on our previous work [8], and in part of the first author's PhD thesis [9], we build upon prior research by incorporating a comprehensive analysis of the equations of state (EoSs) relevant to SDs. This involves a detailed examination of the mass–radius relationship for these objects. Furthermore, we give an explicit mathematical framework that yields a formula for fixing the quark content within the core of an SD.

Additionally, we have broadened our discussion to include potential astrophysical signatures of SDs. This extension is crucial for observational astrophysics, as it may provide insights into identifying and verifying the existence of SDs through observable phenomena.

## 2. Equation of State

One important consideration in assessing the stability of SDs lies in the nature of their EoSs. Historically, when examining this aspect in previous works [3,4,7], the EoS was formulated as follows:

$$\varepsilon(P) = \begin{cases} \varepsilon_{\mathrm{BPS}}(P) & \text{if } P \leq P_{\mathrm{t}} \\ \varepsilon_{\mathrm{quark}}(P) & \text{if } P > P_{\mathrm{t}}\,. \end{cases} \tag{1}$$

In this expression, $\varepsilon_{\mathrm{BPS}}$ represents the Baym–Pethick–Sutherland (BPS) EoS [14], while $\varepsilon_{\mathrm{quark}}$ denotes an EoS characterizing strange quark matter, which can be based on the MIT bag model [15]. The most important parameter in this formulation is the transition pressure $P_{\mathrm{t}}$ (corresponding to the energy density $\varepsilon_{\mathrm{t}}$), which is the pressure at the boundary between quark matter and nuclear matter.

As the EoS for nuclear matter, we use the BPS EoS, which represents the ideal "limit" for WDs in which all elements up to Fe have been produced. This EoS displays a Chandrasekhar mass of approximately 1 $M_{\odot}$, a value lower than the typical Chandrasekhar mass for C-O WDs or O-Mg-Ne WDs (1.4 $M_{\odot}$ and 1.2 $M_{\odot}$). It has been pointed out in work by Benvenuto and Althaus [16] that the use of the BPS EoS is not realistic for WDs. Nevertheless, as will be explained in Section 5.1, it represents the limit in compactness for WDs since it provides the smallest radius for a given mass.

In our work, we use a fit of the BPS EoS in order to avoid artifacts due to the numerical differentiation of a piecewise interpolation. The form of the fit of the BPS EoS is as follows:

$$\varepsilon(P) = e^{f(ln(P))} \tag{2}$$

where the function $f$ is as follows:

$$\begin{aligned} f(x) = &-1496.7952111882255 + 1109.8179718329682\, x^{1/3} \\ &- 171.06847907037277\, x^{4/3} + 95.47548413371702\, x^{5/3} \\ &- 19.652076548674618\, x^{2} + 1.4412357260222872\, x^{7/3} \\ &- 3.995517504571193 \times 10^{-14} x^{8}. \end{aligned} \tag{3}$$

Note that the inclusion of decimal digits is essential for achieving adequate precision across a broad spectrum of pressures and densities. The fit ranges in energy density from $\sim 7$ g/cm$^3$ to $\sim 4 \times 10^{11}$ g/cm$^3$ and it is visible in Figure 1. The percentage error is normally smaller than about 7%, except for a small region at densities of about 20 g/cm$^3$ where the error reaches about 17%.

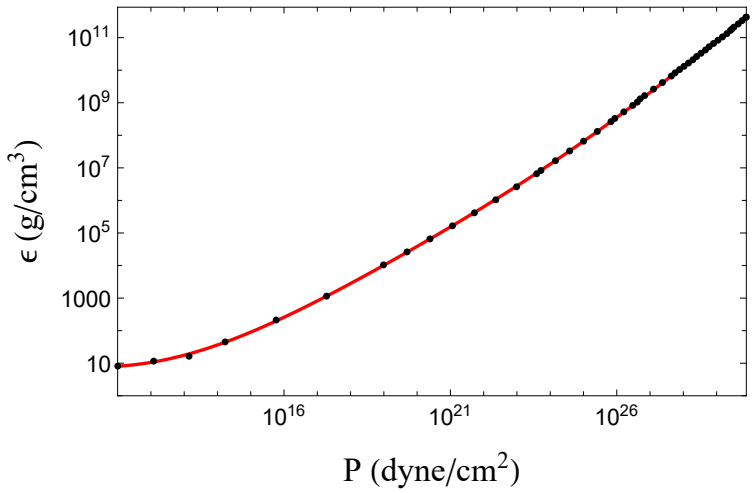


**Figure 1.** BPS equation fit in red, tabulated points in black.

When dealing with SDs, it is important to understand that one can use any value for $\varepsilon_t$ as long as it is less than $\varepsilon_{drip} \approx 4 \times 10^{11}$ g/cm$^3$.

Unlike regular WDs, where one typically only needs to specify the central pressure $P_0$ to define a star's configuration when solving the TOV equation [17], SDs require two parameters. As clear from Equation (1), the first parameter is the transition pressure $P_t$, which represents the pressure at the interface where the quark core meets the outer nuclear matter envelope, the second one is indeed the central pressure as in the normal case $P_0$.

What allows the formation of SDs is the existence of the Coulomb barrier that separates the outer nuclear matter from the inner core of quark matter. This separation occurs when the maximum density of nuclear matter is lower than the neutron drip density $\varepsilon_{drip}$. Beyond this density, free neutrons start to appear. Importantly, since they are not subject to the constraints of the Coulomb barrier, they can readily penetrate the core of quark matter. Upon entering the core, they are absorbed, which leads to the deconfinement of their constituent quarks.

Given that for SDs, the solutions of the TOV depend on two parameters, a question arises about the suitability of choosing the pair of parameters $(P_0, P_t)$ for characterizing these configurations. Choosing a value of $P_t$ does not account for the fact that below the neutron drip density, the baryonic content of the core remains constant, despite changing the central pressure $P_0$. The studies by Vartanyan et al. [18] and Vartanyan et al. [19] discuss the case in which nuclear matter cannot transition into quark matter, allowing for the definition of sequences of SDs with the same quark content in the core, which we define as $B_{core}$. Consequently, one can solve the TOV equation with an alternative parameter pair, namely $(P_0, B_{core})$.

The quark baryon number, represented as $B_{core}$, can be expressed as follows:

$$B_{\text{core}}(P_0, P_t) = \int_0^{R_{\text{core}}} 4\pi r^2 \frac{\rho(r)}{\sqrt{1-2m(r)/r}}\, dr. \tag{4}$$

Here, $\rho$ is the baryon density within the quark core. It is important to note that these two parameter choices are not interchangeable. If one opts to keep $P_t$ constant while varying $P_0$, this leads to changes in $B_{\text{core}}$, implying that hadrons can deconfine into quarks because the change in the core is encoded in the fact that the central pressure is changing by fixing the external pressure of the core $P_t$ (transition pressure). Conversely, when $B_{\text{core}}$ is maintained at a constant value, one necessitates an increase in $P_t$ with higher values of $P_0$. Notice that $R_{\text{core}}$ depends on $P_0$ and $B_{\text{core}}$ in the first case, and on $P_0$ and $P_t$ in the second case.

In order to correctly consider an SD EoS at its equilibrium, we want to choose the parameter pair $(P_0, B_{\text{core}})$. $B_{\text{core}}$ is a function of $P_0$ and $P_t$; therefore, we need to find the inverse relation that, given a choice of $B_{\text{core}}$, gives back the value of $P_t$.

In our analysis, since the core of the system is relatively small, we can reasonably approximate its impact on the gravitational force by using Newtonian physics in a first–order approximation and we will later add a general relativistic correction.

For the EoS governing a small quantity of quark matter within the core, we utilize a parametric expression, as follows:

$$P = (\varepsilon - \varepsilon_{\text{W}})a. \tag{5}$$

Here, the variable $a$ serves as a multiplicative parameter that encompasses various factors, including the bag constant. The term $\varepsilon_{\text{W}}$ corresponds to the Witten density, defined as $\varepsilon_{\text{W}} = \varepsilon(P = 0)$. When considering the Newtonian hydrostatic equilibrium and Equation (5), we obtain the following:

$$a\frac{d\varepsilon}{\varepsilon^2} = -\frac{4\pi}{3} r\, dr. \tag{6}$$

Upon integrating both sides and combining all constants into a single parameter, denoted as $K$, we obtain the following equation:

$$\int_{\varepsilon_0}^{\varepsilon_{\text{W}}} \frac{d\varepsilon}{\varepsilon^2} = -K \int_0^{R_{\text{core}}} dr\, r. \tag{7}$$

In this equation, $R_{\text{core}}$ represents the radius of the core, and $\varepsilon_0$ denotes the energy density at the center of the system. The solution to both sides of this equation leads us to the following expression:

$$\varepsilon_0 = \frac{\varepsilon_{\text{W}}}{1 - K\varepsilon_{\text{W}} R_{\text{core}}^2}. \tag{8}$$

This equation shows how the central energy density is connected to the Witten density $\varepsilon_{\text{W}}$, considering the parameter $K$ and the core radius $R_{\text{core}}$.

We can modify Equation (8) to replace the core radius $R_{\text{core}}$ with its baryon content, denoted as $B_{\text{core}}$, since $R_{\text{core}}^2 \propto B_{\text{core}}^{2/3}$. Additionally, considering that our core experiences slight compression due to the surrounding nuclear matter, we can replace $\varepsilon_{\text{W}}$ with the effective energy density specific to the quark core, denoted as $\varepsilon_{\text{t}}^{\text{Q}}$, which is slightly greater than $\varepsilon_{\text{W}}$. Indeed, the transition density at the boundary of the quark core satisfies $\varepsilon_{\text{t}}^{\text{Q}} \geq \varepsilon_{\text{W}}$. The new form of the equation reads as follows:

$$\varepsilon_0(B_{\text{core}}) = \frac{\varepsilon_{\text{t}}^{\text{Q}}}{1 - K\varepsilon_{\text{t}}^{\text{Q}} B_{\text{core}}^{2/3}}. \tag{9}$$

Now, it is reasonable to incorporate some higher–order corrections into Equation (9) to account for general relativistic effects:

$$\varepsilon_0(B_{\rm core}) = \frac{\varepsilon_{\rm t}^{\rm Q}}{1 - k_1 \varepsilon_{\rm t}^{\rm Q} B_{\rm core}^{2/3} - k_2 \varepsilon_{\rm t}^{\rm Q} B_{\rm core}^{4/3}}. \tag{10}$$

In this modified equation, we introduce two numerical parameters, $k_1$ and $k_2$, to account for these higher–order relativistic effects. These parameters are determined numerically and they depend on the quark matter EoS.

For the quark matter, we utilize the following thermodynamic potential [20–22]:

$$\Omega(\mu) = -\frac{3}{4\pi^2} a_4 \, \mu^4 + \frac{3}{4\pi^2}(m_s^2 - 4\Delta_0^2)\mu^2 + B. \tag{11}$$

Here, $a_4 = 0.7$ is a parametrization of perturbative QCD corrections, the gap parameter $\Delta_0$ = 80 MeV, the strange quark mass $m_s$ = 120 MeV, and the bag constant $B = 135^4$ MeV$^4$, as in work by Bombaci et al. [23]. The specific parameter choices allow us to reach maximum masses for an SQS of about 2.6 $M_\odot$.

It is important to note that the parameters $k_1$ and $k_2$ are primarily influenced by the bag constant, and any reasonable adjustments made to the other parameters in Equation (11) have negligible impacts on $k_1$ and $k_2$.

*Mass–Radius Relation*

The relationship between mass and radius exhibits notable differences depending on whether we consider the parameter pairs $(P_0, P_{\rm t})$ or $(P_0, B_{\rm core})$. When constructing a mass–radius (MR) diagram, it is essential to vary one parameter, typically the central pressure (or central energy density), while keeping the other parameters constant.

If we opt to fix the transition pressure $P_{\rm t}$, we are essentially exploring configurations where quark matter consistently appears at the same energy density threshold. We begin with a configuration, where $P_0 = P_{\rm t}$, denoted as point $b$ (or $b'$ and $b''$ depending on the transition energy density), as illustrated in Figure 2. Then, we progress along the bottom branch in a clockwise direction, increasing the central pressure. Point $a$ indicates the Chandrasekhar mass of the WD, while $c$ is the maximum mass for SDs with $\varepsilon_{\rm t} = \varepsilon_{\rm drip}$. The mechanically stable configurations are the ones to the right of $c$.

In Figure 2, it becomes clear how the final point of the MR of the BPS EoS (WD), defined as the point at which $\varepsilon_0 = \varepsilon_{\rm drip}$, joins with the curve obtained by fixing $\varepsilon_{\rm t} = \varepsilon_{\rm drip}$. Indeed, the SD curves, constructed by choosing $P_{\rm t}$ as the transition pressure, join exactly with the WDs' MR at the point where, for the BPS, $P_0 = P_{\rm t}$ (or $\varepsilon_0 = \varepsilon_{\rm t}$). When the transition density is relatively low, the point where the curves join falls before reaching the WDs' maximum mass on the MR diagram (point $a$ in Figure 2). This is evident in Figure 3, where a low energy transition density ($\varepsilon_{\rm t} = 10^7$ g/cm$^3$) is represented by the dashed black curve, which has its maximum allowed mass at approximately 0.5 $M_\odot$; this is where it joins the WD curve, which is not shown in the figure.

On the other hand, the MR relation for SDs tends to converge with that of an SQS when considering small radii. In particular, if the value of $\varepsilon_{\rm t}(P_{\rm t})$ is significantly smaller than the neutron drip density, it implies that there is insufficient matter above the quark core (which now constitutes the majority of the star) to exert significant compression on it. For the high values of $\varepsilon_{\rm t}(P_{\rm t})$, specifically the neutron drip density, the radii of SDs are slightly smaller compared to those of an SQS. This occurs because there is a broader range of pressure that nuclear matter must cover in these cases. This behavior is shown in Figure 4, with detailed representations of the maxima in Figure 5 and the low–mass region in Figure 6.

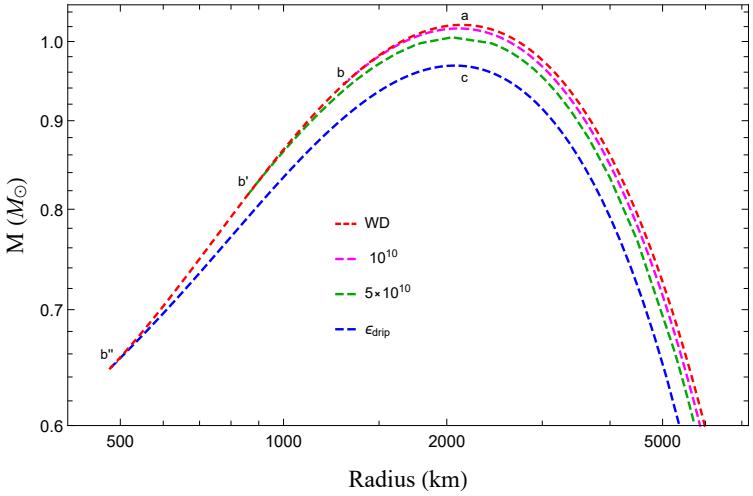


**Figure 2.** Enlarged view of the MR sequence [8] around the Chandrasekhar limit. Additionally, the WD configuration is shown for comparison.

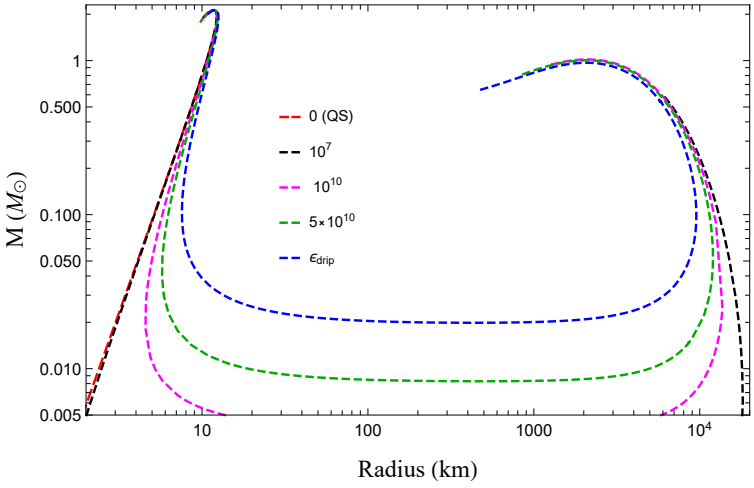


**Figure 3.** MR diagram for EoSs with fixed transition densities, indicated in the legend in units of g/cm$^3$. Also shown in dashed red is the curve for a bare SQS, which does not have a transition density to nuclear matter.

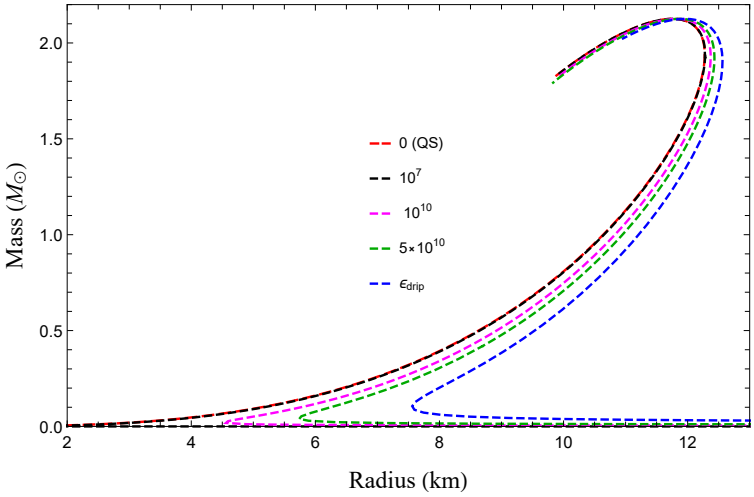


**Figure 4.** Details of Figure 3. Here, the SQS branch is visible, where EoSs with constant $\varepsilon_t$ are analogous to non-bare SQSs, namely SQSs with a nuclear crust.

When we fix $\varepsilon_t(P_t)$, we implicitly let $B_{core}$ vary. Conversely, when we fix the baryon content of the core ($B_{core}$), it is the transition density that changes along the diagram.

When we establish a fixed value for $B_{core}$, the corresponding configuration contains a specific quantity of quarks in its core. If we start from a point at which $\varepsilon_t(P_t) = 0$, there is no nuclear matter situated above the core to exert compression. In other words, it corresponds to the extreme point on the left side of Figure 3 (red dashed curve) and satisfies Equation (8).

As we increase the central energy density (which means adding nuclear matter on top of the quark core), we move in a counter-clockwise direction on the MR diagram. During this progression, we intersect curves in Figure 3 that correspond to increasing values of $\varepsilon_t(P_t)$. This means that a curve representing a constant $B_{core}$ is comprised of configurations with varying $\varepsilon_t(P_t)$. The initial point on this curve has $\varepsilon_t = 0$ (or equivalently $\varepsilon_t^Q = \varepsilon_W$), while the final point corresponds to $\varepsilon_t = \varepsilon_{drip}$.

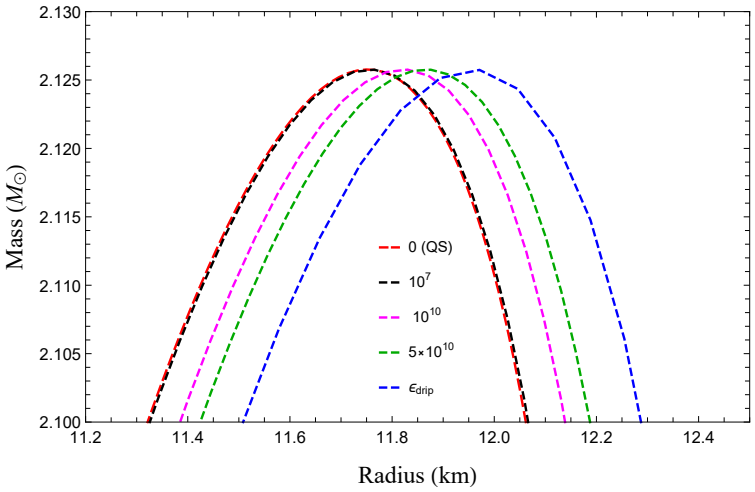


**Figure 5.** Magnification of the maxima in Figure 4. The higher the transition density of the nuclear matter, the more compact the star. Indeed, the wider the range between the constant $\varepsilon_t$ and the star's surface, the greater the compression exerted by the surrounding nuclear matter on the strange core.

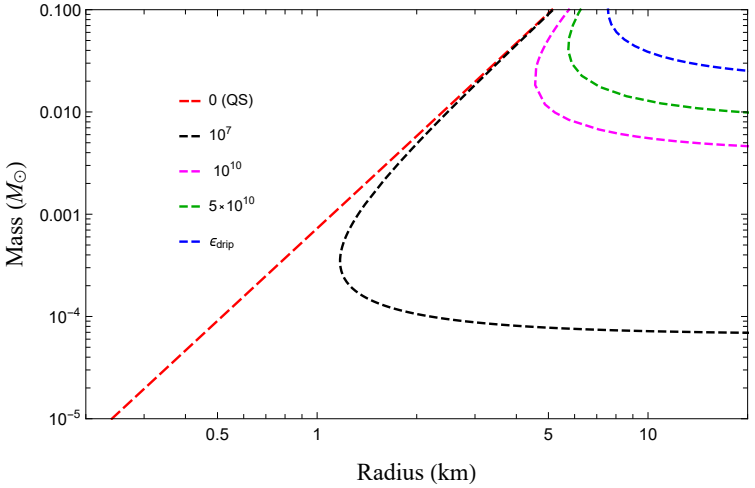


**Figure 6.** A closer look at the low–mass stars in Figure 4. It is evident that when $\varepsilon_t$ is low, the deviation from the radius of an SQS is less pronounced.

In Figure 7, we can observe specific behavior where, if the value of $B_{core}$ is too large, the condition $\varepsilon_t = \varepsilon_{drip}$ is achieved at relatively small radii. The extreme points belong to the curve representing the highest possible density of nuclear matter within the star, which corresponds to the neutron drip density (the blue dashed one).

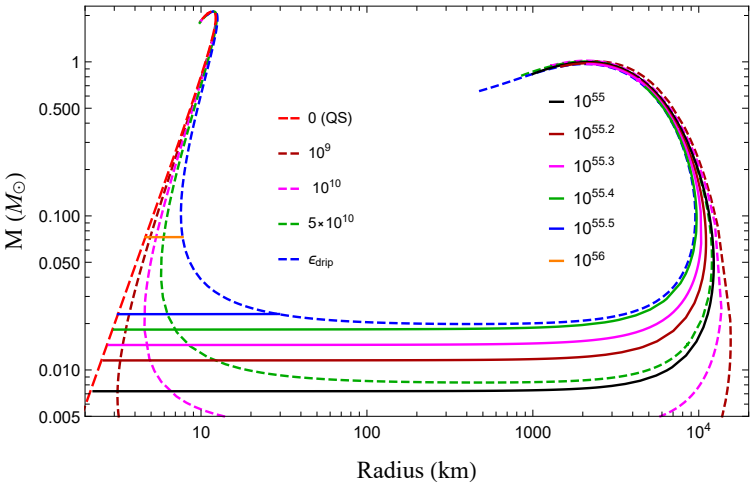


**Figure 7.** MR sequences of SDs from Di Clemente et al. [8]. Configurations with constant transition pressure $P_t$ are represented by dashed lines. As the central pressure $P_0$, namely $B_{\rm core}$, increases, these sequences progress in a clockwise direction. The corresponding values of the transition density $\varepsilon_t$, measured in g/cm$^3$, are specified in the legend. Conversely, solid lines depict configurations where the quark content of the core, $B_{\rm core}$, remains unchanged. In this scenario, increasing $P_0$ (therefore, increasing $P_t$) makes the curves progress anti–clockwise. In this case, the legend indicates the specific values of $B_{\rm core}$.

## 3. Radial Oscillations

Radial oscillations are tools that can be used to assess the stability of a star. The equation for radial oscillations is derived by perturbing both the fluid variables and the spacetime metrics that characterize the interior of the star.

The differential equation governing radial oscillations can be expressed as follows:

$$(H\xi')' = -(\omega^2 W + Q)\xi\,. \tag{12}$$

Here, $\xi(r)$ represents the rescaled radial Lagrangian displacement [13], while $\omega$ is the frequency of the oscillation mode. The functions in Equation (12) are defined as follows:

$$\begin{aligned} H &= r^{-2}(\varepsilon + P)e^{\lambda+3\phi}c_s^2 \\ Q &= r^{-2}(\varepsilon + P)e^{\lambda+3\phi}(\phi'^2 + 4r^{-1}\phi' - 8\pi e^{2\lambda}P) \\ W &= r^{-2}(\varepsilon + P)e^{3\lambda+\phi}\,. \end{aligned} \tag{13}$$

Here, $c_s^2$ represents the speed of sound, while $\lambda(r)$ and $\phi(r)$ are the metric potentials. It is essential to note that when dealing with multiple layers or phase transitions within the star, it becomes necessary to establish clear boundary conditions at the interfaces between these layers [10]. One must specify whether the two components of the fluid can transition into one another, within the timescale of the oscillation. This consideration depends on the presence of phase transitions and their associated timescales. Therefore, we categorize these transitions as either *slow transitions* or *fast transitions* to distinguish between their characteristic timescale.

### 3.1. Slow Transition

The scenario of a slow phase transition refers to a situation in which the timescale for the conversion is significantly longer than the timescale of the perturbation. In this scenario, the two phases do not intermix during the oscillations, and the volume element near the surface that separates the phases moves along with the interface, expanding and contracting. This particular situation applies to SDs where $\varepsilon_{\rm t} < \varepsilon_{\rm drip}$, which essentially means that the two phases never mix. In other words, we are considering the stability of star configurations on the MR diagram where $B_{\rm core}$ remains constant, as it cannot increase. In a practical sense,

each star configuration can be associated with either a curve characterized by $B_{\rm core}$ or one defined by $P_{\rm t}$ but only one of them is physically acceptable. Consequently, the choice of boundary conditions for radial oscillations must align with this physical interpretation.

For the slow conversion, the interface conditions involve the continuity of the radial displacement at the boundary $r_{\rm t}$:

$$[\xi]^{+}_{-} \equiv \xi(r_{\rm t}^{+}) - \xi(r_{\rm t}^{-}) = 0\,. \tag{14}$$

Additionally, it requires ensuring the continuity of the Lagrangian perturbation of pressure:

$$[\Delta P]^{+}_{-} = \left[-e^{\phi}\, r^{-2}\, \gamma(r)\, P\, \frac{\partial \xi}{\partial r}\right]^{+}_{-} = 0\,. \tag{15}$$

Here, $\gamma(r)$ represents the relativistic adiabatic index, given by $\gamma(r) = (\partial P/\partial \varepsilon)(\varepsilon + P)P^{-1}$. By solving Equation (12), $\omega^2 > 0$ approaches the zero value at the maximum mass in the MR plane along the curve defined by the constant values of $B_{\rm core}$, as proposed by the criteria of Zel'dovich [12] and Bardeen et al. [13]. The eigenfunctions exhibit continuity with a kink at $r_{\rm t}$ (as shown in Figure 8), and the same behavior is reflected in $\Delta P(r)$ [11].

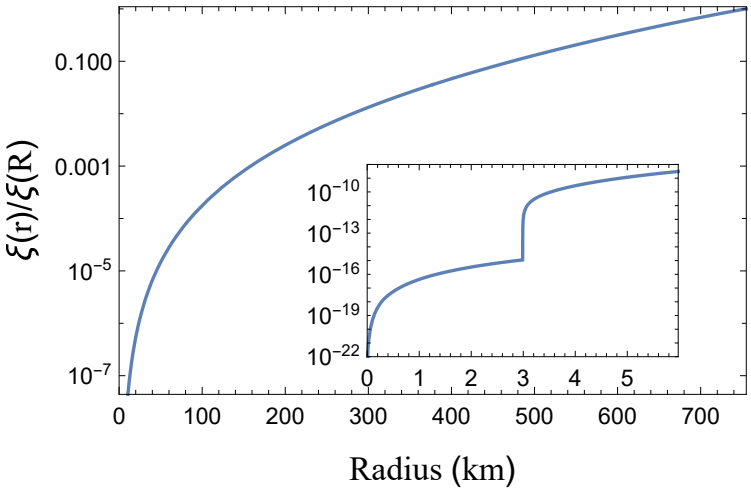


**Figure 8.** In the scenario where hadronic matter does not transition into quark matter during the oscillation timescale, the fundamental eigenfunction of radial modes is examined. The star under consideration in this analysis and referred to in the fast scenario figure has $\mathrm{M} \simeq 0.02\,\mathrm{M}_{\odot}$, $B_{\rm core} \simeq 2.69 \times 10^{55}$ and $\varepsilon_t = \varepsilon_{\rm drip}$. This strange dwarf is situated just beyond the minimum point on the dashed blue curve in Figure 7. The mode in question is stable since $\omega^2 = 0.788275\,\mathrm{Hz}^2$ is positive. A closer look at the region near $r = r_t$ within the inset plot highlights a kink in the eigenfunction. Figure borrowed from Di Clemente et al. [8].

### *3.2. Rapid Transition*

It is possible to exchange mass between the two phases when the timescale for the conversion is shorter than the timescale of the perturbation. The boundary between these phases is in thermodynamic equilibrium, given the rapid conversion rates; therefore, Equation (15) remains applicable in this scenario.

The difference with respect to the slow transition case is in the interface condition from Equation (14). Here, this condition becomes as follows:

$$\left[\xi + \frac{\gamma P \xi'}{P'}\right]^{+}_{-} = 0. \tag{16}$$

This modification results in an eigenfunction that exhibits a discontinuity at the interface, distinguishing it from the behavior seen in slow transitions, as visible when comparing Figure 9 and Figure 8.

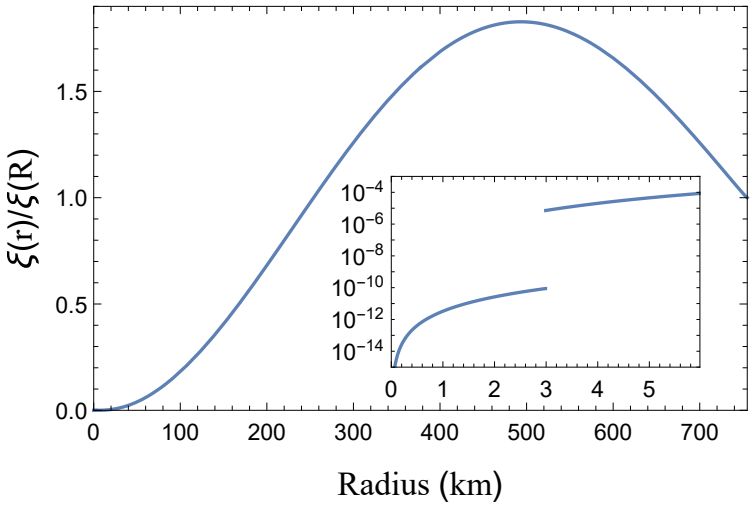


**Figure 9.** In the rapid transition scenario, we observe a fundamental eigenfunction that has a sharp discontinuity, suggesting an instantaneous change rather than a gradual one, even though it is extremely rapid in work by Alford et al. [7]. This mode is unstable since it is characterized by a negative squared frequency of $\omega^2 = -1.62785\,\mathrm{Hz}^2$. Figure borrowed from Di Clemente et al. [8].

The reason behind the apparent inconsistency between the findings of Glendenning et al. [3,4] and those of Alford et al. [7] is now evident. In the work of Alford et al. [7], they employed an EoS similar to the one discussed in Equation (1). However, they introduced a smoothing mechanism that eliminated the sharp discontinuity between the two phases, which notably, allowed for an instantaneous transformation from one phase to the other for the oscillation timescale. The smoothed EoS used in [7] can be written as follows:

$$\begin{aligned}\varepsilon(P) = {} & [1 - \tanh((P - P_{\mathrm{crit}})/\delta P)\varepsilon_{\mathrm{BPS}}(P)]/2 \\ & + \left[1 + \tanh((P - P_{\mathrm{crit}})/\delta P)\varepsilon_{\mathrm{quark}}(P)\right]/2\,. \end{aligned} \tag{17}$$

Here, $\delta P$ represents the transition width. This approach is analogous to the rapid transition case discussed here as both implicitly allow for a mixed phase. In [7], the eigenfunction exhibits a very rapid increase at the interface without a proper discontinuity. The magnitude of this increase is entirely equivalent to the magnitude of the discontinuity we obtain, which is illustrated in Figure 9.

In contrast, it is possible that, in work by Glendenning et al. [3,4], the eigenfunction is assumed to be continuous, corresponding to the situation described in the slow transition scenario.

The distinction between slow and rapid transitions introduced by Thorne [24] is based on the observation that the consistency between stability analyses, one based on the TOV solutions and the other on radial oscillations, is linked to the use of the adiabatic index derived from the EoS employed in the static analysis. The analyses coincide in the case of rapid transitions. In contrast, in slow transitions, it is generally challenging to calculate the adiabatic index, primarily due to the need to account for imbalances introduced by perturbations in the computation of the slow adiabatic index [25,26].

In our case, the conversion between hadrons and quarks is confined to a two–dimensional surface, rather than an extended volume. This simplifies the modification of both the adiabatic index since it corresponds to adapting the interface conditions [10], and the EoS. In the context of the slow transition scenario, this means to fix the quark content [18,19]. This dual modification allows the creation of a link between static and dynamic analyses in the case of slow transitions. This relationship is shown in Figure 10. It is worth noting that this correspondence was already established by Alford et al. [7] in the context of the rapid transition case and we reproduced the behavior near the minimum in Figure 11.

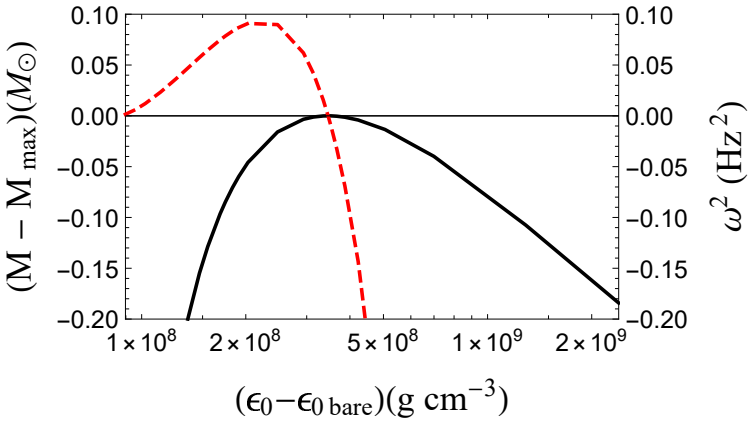


**Figure 10.** Eigenvalues of the fundamental mode for the slow scenario are depicted by a dashed line, whereas the solid line represents the masses of SDs with a core baryonic content $B_{\rm core} = 10^{55}$, approaching the Chandrasekhar mass $M_{\rm max} \approx 0.996\ M_{\odot}$. These are plotted as functions of the central energy density, $\epsilon_0$ shifted by a constant factor $\epsilon_{0\ \rm bare}$, which is a pure QS sharing the same $B_{\rm core}$. The point where $\omega^2$ becomes zero aligns with the maximum mass, beyond which $\omega^2$ turns negative, indicating instability at higher densities. The figure is borrowed from Di Clemente et al. [8].

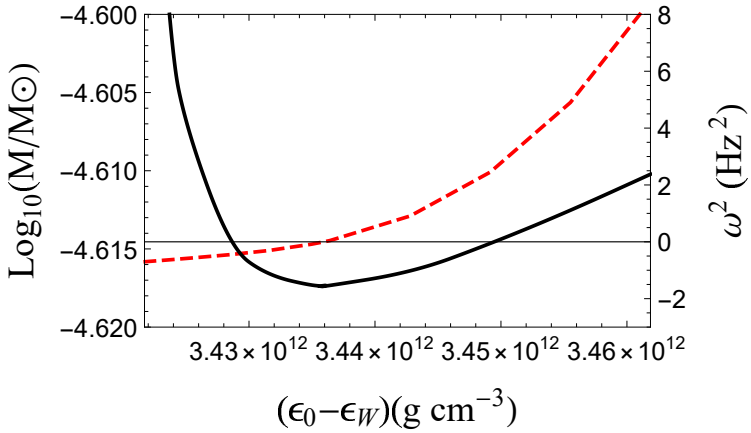


**Figure 11.** Eigenvalues of the fundamental mode in the fast case (dashed) and masses of SDs having $\varepsilon_t = \varepsilon_{\rm drip}$, close to the minimum (solid), plotted as functions of the difference between the central energy density, $\epsilon_0$, and the Witten one, $\epsilon_{\rm W}$. The zero of $\omega^2$ coincides with the minimum mass. This result is consistent with [7].

The results on the stability of SDs, obtained in work by Di Clemente et al. [8] and summarized here, were later confirmed by the analysis of Goncalves et al. [27].

## 4. SD Collapse

The transition from ordinary matter to strange quark matter can release huge amounts of energy and it can be associated with violent phenomena such as gamma–ray bursts [28–30] and extremely energetic supernovae [31]. In this review, we will only discuss the possible transition of ordinary matter in an SD to strange quark matter and we will discuss its possible signatures. In a binary system where a WD orbits a main sequence star, mass transfer occurs as the WD accretes material from its companion. This typical scenario culminates in a type Ia supernova (SN) event. However, a different outcome known as accretion–induced collapse (AIC) is theoretically possible. It is important to note that while the concept of AIC has been explored, actual observations of such events are notably absent [32]. This absence can be attributed to the substantial difference in timescales between the collapse process and the nuclear reactions responsible for igniting the WD deflagration.

The presence of the strange quark matter core in SDs becomes important when the object faces significant perturbations, like in the early stages of a type Ia supernova (SN)

event. Specifically, if the quark matter core is sufficiently large, it can potentially cause the object to collapse rather than undergo the usual deflagration process (see the illustration in Figure 12). The difficulties of achieving an AIC arise from the fact that nuclear reactions occur when the star is near the Chandrasekhar limit. This phase, characterized by marginal mechanical stability ($\omega^2 \simeq 0$), leads to the star's disruption before AIC can take place [33].

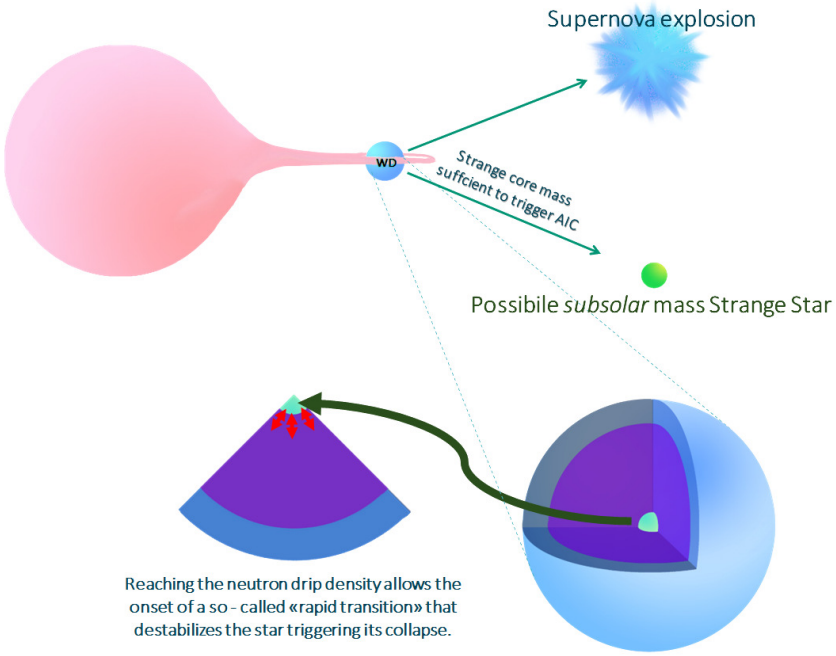


**Figure 12.** Illustration of the AIC mechanism for a system consisting of an SD and a main sequence star.

The mechanical instability of SDs is strictly related to the rapid conversion of hadrons into quarks. This process is a crucial mechanism that allows the star to undergo a collapse by becoming mechanically unstable.

As long as $\varepsilon_t \ll \varepsilon_{drip}$, the object remains mechanically stable. However, the system becomes unstable if a fluctuation causes the density to exceed $\varepsilon_{drip}$ in a small region near the core or if free neutrons are produced and fall into the quark core. In this analysis, temperature can play an important role. From Haensel et al. [34] and Hempel and Schaffner-Bielich [35], one can notice that at temperatures exceeding about 0.5 MeV, a significant fraction of free neutrons appears, already at densities of the order of $10^9$ g/cm$^3$. To assess this instability, we calculate the fundamental eigenvalue of a star at the Chandrasekhar limit, assuming $B_{core}$ remains constant. While for a slow transition, $\omega^2 = 0$, in the case of a rapid transition, for the same point in the MR diagram, $\omega^2$ becomes significantly negative. It is important to remark that each point at constant $B_{core}$ corresponds to a point at constant $\varepsilon_t$; therefore, one can go from a situation in which the transition is physically slow to a situation in which the star's internal boundary is in a rapid transition regime and the baryon content of the core is not constant anymore. In any case, it is illogical to apply a slow transition scenario when $\varepsilon_t$ remains constant or to employ a fast transition scenario when $B_{core}$ is held constant because $B_{core}$ cannot increase in that case (and, therefore, the transition must not occur). However, exceptions may arise when the star is in close proximity to the Chandrasekhar mass. In such situations, perturbations could potentially drive a small region of the star, located near the strange core, to exceed the neutron drip density or generate some free neutrons. This, in turn, could trigger the phase transition, going from having a constant $B_{core}$ to a situation in which $B_{core}$ increases because of the neutron flux.

Figure 13 displays the e–folding time, defined as $2\pi/|\omega|$. When $B_{core} \gtrsim 10^{46}$, the e–folding, which is the typical collapse timescale, falls below 1 second, implying that the collapse can be more rapid than the full development of a deflagration, which is of the order of several seconds [36]. It can be argued that the amount of quark matter that triggers

the collapse depends on the EoS. Therefore, we calculated the e–folding time for the set of parameters for the quark EoS presented in work by Bombaci et al. [23]. The results remained consistent with our previous findings. In the same figure, the maximum density reached by the nuclear matter component at the boundary ($\varepsilon_t$) is also shown. From the behavior of $\varepsilon_t$, it is possible to determine when the static structure of a 1 $M_\odot$ SD remains similar to the one of a WD. When $B_{\rm core} \gtrsim 10^{52}$, the structure of the star changes, and the boundary density $\varepsilon_t$ deviates from $\sim 10^9$ g/cm$^3$, which is the typical central density of a WD at the Chandrasekhar mass. This suggests that the presence of the quark core does not influence the static properties of the star unless the value of $B_{\rm core}$ is large enough to exert a noticeable gravitational pull.

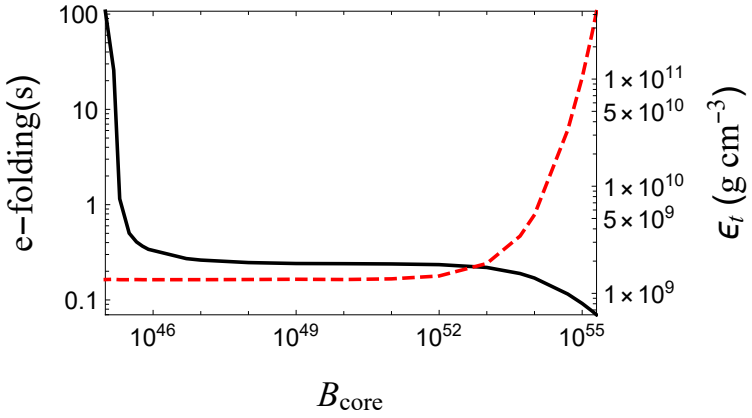


**Figure 13.** The characteristics of stars at their maximum mass are analyzed in relation to their quark content. The solid black curve represents how the timescale of mechanical instability varies with $B_{\rm core}$. Meanwhile, the dashed red line illustrates the density at which the transition occurs, highlighting the relationship between the core's baryonic content and the WD's structural stability. Figure borrowed from Di Clemente et al. [8].

An essential query regarding SDs pertains concerns how they accumulate the strange quark matter in their cores. The most straightforward explanation lies in the idea that WDs gradually accumulate strangelets over their lifespan. This idea is linked to the possibility that dark matter is made, at least in part, of strangelets [6]. In a few papers, it has been shown that this scenario is compatible with the most recent data from cosmology and astrophysics [37–40]. In work by Di Clemente et al. [41], we have shown that an astrophysical path leading to the formation of subsolar compact stars in electron-capture supernovae can be based on the hypothesis of dark matter made of strangelets. The existence of subsolar-mass compact objects has been suggested in work by Doroshenko et al. [42] and it cannot be explained by solely considering standard equations of state [43].

Another mechanism to produce subsolar-mass compact objects is based on AIC. If AIC takes place in an SD instead of a WD, an SQS is produced instead of an NS. Since this phenomenon is very energetic and the collapsed object is more bound than NSs, the final object can be a subsolar-mass km-sized compact star [8,44].

## 5. Other Signatures

A novel approach to distinguish SDs from WDs (by utilizing gravitational-wave observations, specifically by measuring the tidal deformability) was suggested in work by Perot et al. [45].

When comparing SDs to WDs, a notable feature is the significant reduction in the tidal deformability coefficient, which can reach up to 50% for an SD with a mass of 0.6 $M_\odot$. This difference in tidal parameters could be measured by upcoming space-based gravitational-wave detectors such as the laser interferometer space antenna (LISA).

In work by Perot et al. [45], the authors do not employ the BPS EoS to describe the WD structure. Instead, they utilize a more refined EoS that accounts for the precise atomic species and their correct balance within the WDs. Additionally, pycnonuclear reactions are taken into account, which usually have their onset at a density of $10^{10}$ g/cm$^3$ for the carbon layer, so at a density of interest for SDs. Nevertheless, their analysis indicates that the impact of these reactions is minimal on the SD structure.

Perot and Chamel [46] on the other hand, focused on the effect of having a crystalline color superconductor [47] as the phase for the strange quark matter core. The effect of the large rigidity of the elastic core on the tidal deformability should be relevant (which has a shear modulus that is 2–3 times larger than the one of the hadronic envelope) but it is totally canceled because of the presence of the surrounding hadronic layers. Nevertheless, the reduction in tidal deformability, compared to that of a white dwarf, remains significant due to the presence of the strange matter core.

### *5.1. Possible SD Observations*

It is worth noting that in a study by Kurban et al. [48], seven potential SD candidates were identified. These candidates exhibit a mass range spanning from approximately 0.02 to 0.12 $M_\odot$ and have relatively consistent radii, falling within the approximate range of 9000 to 15,000 km. To illustrate the incompatibility with WDs models of those candidates, the paper presents MR relationships for WDs using EoSs of pure magnesium (Mg) and helium (He) stars, in addition to the BPS EoS. By employing an EoS for SDs similar to that in work by Alford et al. [7], it is shown how these objects, due to their compactness, can be good SD candidates. Moreover, this claim is supported by the fact that the BPS EoS serves as an upper limit for compactness in WDs.

To identify potential SD candidates, the authors analyzed WDs listed in the Montreal White Dwarf Database[1]. They employed analyses based on spectroscopic data and Gaia observations [49]. The data points with their error bars corresponding to the objects identified as SD candidates are visible in Figure 14.

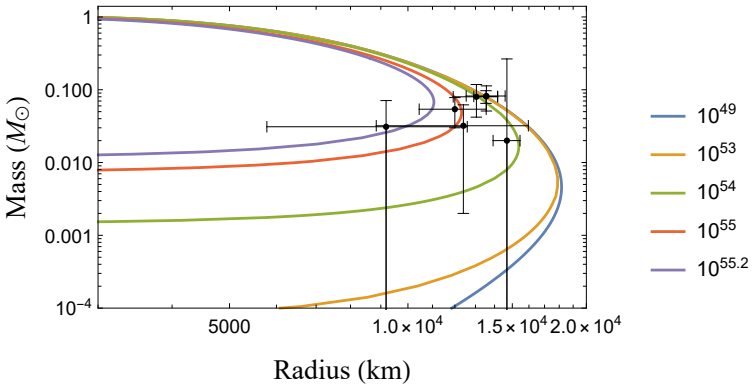


**Figure 14.** MR relation for constant $B_{\text{core}}$ SDs with data from the Kurban et al. [48] analysis.

Recent and more precise measurements of the masses and radii of these WDs by the satellite GAIA [50] indicate that some of these objects could be compatible with a normal WD scenario.

## 6. Conclusions

The existence of strange dwarfs is an intriguing possibility in astrophysics since it is strictly connected to cosmology and, in particular, to the possibility that dark matter is composed of nuggets of strangelets [6,40]. One of the most profound astrophysical consequences of the existence of strange dwarfs involves the potential formation of subsolar SQSs [8]. This formation process could occur through an accretion-induced collapse mechanism. However, the feasibility and specific mechanisms at the basis of this process require further investigation, potentially through detailed studies and simulations in the future.

**Author Contributions:** Conceptualization, F.D.C., A.D. and G.P.; formal analysis, F.D.C., A.D. and G.P.; writing—original draft preparation, F.D.C., A.D. and G.P.; writing—review and editing, F.D.C., A.D. and G.P. All authors have read and agreed to the published version of the manuscript.

**Funding:** This research received no external funding.

**Data Availability Statement:** Data are contained within the article.

**Conflicts of Interest:** The authors declare no conflicts of interest.

## Abbreviations

The following abbreviations are used in this manuscript:

| | |
|---|---|
| NS | neutron star |
| SQS | strange quark star |
| WD | white dwarf |
| SD | strange dwarf |
| MR | mass-radius |
| EoS | equation of state |
| TOV | Tolman–Oppenheimer–Volkoff |
| BPS | Baym–Pethick–Sutherland |
| SN | supernova |
| AIC | accretion-induced collapse |

## Note

[1] http://www.montrealwhitedwarfdatabase.org/tables-and-charts.html (accessed on 1 October 2023).

## References

1. Heger, A.; Fryer, C.L.; Woosley, S.E.; Langer, N.; Hartmann, D.H. How massive single stars end their life. *Astrophys. J.* **2003**, *591*, 288–300. [CrossRef]
2. Chandrasekhar, S. The maximum mass of ideal white dwarfs. *Astrophys. J.* **1931**, *74*, 81–82. [CrossRef]
3. Glendenning, N.K.; Kettner, C.; Weber, F. A Possible new class of dense white dwarfs. *Phys. Rev. Lett.* **1995**, *74*, 3519–3521. [CrossRef] [PubMed]
4. Glendenning, N.K.; Kettner, C.; Weber, F. From strange stars to strange dwarfs. *Astrophys. J.* **1995**, *450*, 253–261. [CrossRef]
5. Bodmer, A.R. Collapsed nuclei. *Phys. Rev. D* **1971**, *4*, 1601–1606. [CrossRef]
6. Witten, E. Cosmic Separation of Phases. *Phys. Rev. D* **1984**, *30*, 272–285. [CrossRef]
7. Alford, M.G.; Harris, S.P.; Sachdeva, P.S. On the stability of strange dwarf hybrid stars. *Astrophys. J.* **2017**, *847*, 109. [CrossRef]
8. Di Clemente, F.; Drago, A.; Char, P.; Pagliara, G. Stability and instability of strange dwarfs. *Astron. Astrophys.* **2023**, *678*, L1. [CrossRef]
9. Di Clemente, F. Strange Quark Matter in Astrophysics and Cosmology. Ph.D. Thesis, Department of Physics and Earth Science, University of Ferrara, Ferrara, Italy, 2024.
10. Pereira, J.P.; Flores, C.V.; Lugones, G. Phase transition effects on the dynamical stability of hybrid neutron stars. *Astrophys. J.* **2018**, *860*, 12. [CrossRef]
11. Di Clemente, F.; Mannarelli, M.; Tonelli, F. Reliable description of the radial oscillations of compact stars. *Phys. Rev. D* **2020**, *101*, 103003. [CrossRef]
12. Zel'dovič, J.B.; Novikov, I.D. Reljativistskaja astrofizika. I. *Uspehi Fizičeskih Nauk* **1964**, *84*, 377–417. Available online: https://ufn.ru/ufn64/ufn64_11/Russian/r6411a.pdf (accessed on 1 October 2023). [CrossRef]
13. Bardeen, J.M.; Thorne, K.S.; Meltzer, D.W. A Catalogue of Methods for Studying the Normal Modes of Radial Pulsation of General-Relativistic Stellar Models. *Astrophys. J.* **1966**, *145*, 505. [CrossRef]
14. Baym, G.; Pethick, C.; Sutherland, P. The Ground state of matter at high densities: Equation of state and stellar models. *Astrophys. J.* **1971**, *170*, 299–317. [CrossRef]
15. Chodos, A.; Jaffe, R.L.; Johnson, K.; Thorn, C.B.; Weisskopf, V.F. New extended model of hadrons. *Phys. Rev. D* **1974**, *9*, 3471–3495. [CrossRef]
16. Benvenuto, O.G.; Althaus, L.G. The Structure and Thermal Evolution of Strange Dwarf Stars. *Astrophys. J.* **1996**, *462*, 364. [CrossRef]

17. Oppenheimer, J.R.; Volkoff, G.M. On massive neutron cores. *Phys. Rev.* **1939**, *55*, 374–381. [CrossRef]
18. Vartanyan, Y.L.; Hajyan, G.S.; Grigoryan, A.K.; Sarkisyan, T.R. Stability of strange dwarfs I: Static criterion for stability. Statement of the problem. *Astrophysics* **2009**, *52*, 300–306. [CrossRef]
19. Vartanyan, Y.L.; Hajyan, G.S.; Grigoryan, A.K.; Sarkisyan, T.R. Stability valley for strange dwarfs. *Astrophysics* **2012**, *55*, 98–109. [CrossRef]
20. Alford, M.; Braby, M.; Paris, M.W.; Reddy, S. Hybrid stars that masquerade as neutron stars. *Astrophys. J.* **2005**, *629*, 969–978. [CrossRef]
21. Weissenborn, S.; Sagert, I.; Pagliara, G.; Hempel, M.; Schaffner-Bielich, J. Quark Matter in Massive Neutron Stars. *Astrophys. J. Lett.* **2011**, *740*, L14. [CrossRef]
22. Zhang, C.; Gammon, M.; Mann, R.B. Stellar structure and stability of charged interacting quark stars and their scaling behavior. *Phys. Rev. D* **2021**, *104*, 123007. [CrossRef]
23. Bombaci, I.; Drago, A.; Logoteta, D.; Pagliara, G.; Vidaña, I. Was GW190814 a Black Hole–Strange Quark Star System? *Phys. Rev. Lett.* **2021**, *126*, 162702. [CrossRef] [PubMed]
24. Thorne, K.S. The General-Relativistic Theory of Stellar Structure and Dynamics. In *The General-Relativistic Theory of Stellar Structure and Dynamics, Proceedings of the International School of Physics Enrico Fermi. Course XXXV, Varenna, Italy, 12–24 July 1965*; Academic Press: New York, NY, USA, 1966; pp. 166–280.
25. Lindblom, L.; Owen, B.J. Effect of hyperon bulk viscosity on neutron star r modes. *Phys. Rev. D* **2002**, *65*, 063006. [CrossRef]
26. Drago, A.; Lavagno, A.; Pagliara, G. Bulk viscosity in hybrid stars. *Phys. Rev. D* **2005**, *71*, 103004. [CrossRef]
27. Goncalves, V.P.; Jimenez, J.C.; Lazzari, L. Revisiting the stability of strange-dwarf stars and strange planets. *Eur. Phys. J. A* **2023**, *59*, 251. [CrossRef]
28. Bombaci, I.; Datta, B. Conversion of neutron stars to strange stars as the central engine of gamma-ray bursts. *Astrophys. J. Lett.* **2000**, *530*, L69. [CrossRef] [PubMed]
29. Ouyed, R.; Dey, J.; Dey, M. Quark - nova as gamma-ray burst precursor. *Astron. Astrophys.* **2002**, *390*, L39. [CrossRef]
30. Berezhiani, Z.; Bombaci, I.; Drago, A.; Frontera, F.; Lavagno, A. Gamma-ray bursts from delayed collapse of neutron stars to quark matter stars. *Astrophys. J.* **2003**, *586*, 1250–1253. [CrossRef]
31. Leahy, D.; Ouyed, R. Supernova SN2006gy as a first ever Quark Nova? *Mon. Not. R. Astron. Soc.* **2008**, *387*, 1193. [CrossRef]
32. Wang, B.; Liu, D. The formation of neutron star systems through accretion-induced collapse in white-dwarf binaries. *Res. Astron. Astrophys.* **2020**, *20*, 135. [CrossRef]
33. Canal, R.; Isern, J.; Labay, J. The origin of neutron stars in binary systems. *Ann. Rev. Astron. Astrophys.* **1990**, *28*, 183–214. [CrossRef]
34. Haensel, P.; Kaminker, A.; Yakovlev, D. Electron neutrino-antineutrino bremsstrahlung in a liquid phase of neutron star crusts. *Astron. Astrophys.* **1996**, *314*, 328–340. [CrossRef]
35. Hempel, M.; Schaffner-Bielich, J. A statistical model for a complete supernova equation of state. *Nuclear Phys. A* **2010**, *837*, 210–254. [CrossRef]
36. Gamezo, V.N.; Khokhlov, A.M.; Oran, E.S.; Chtchelkanova, A.Y.; Rosenberg, R.O. Thermonuclear supernovae: Simulations of the deflagration stage and their implications. *Science* **2003**, *299*, 77. [CrossRef] [PubMed]
37. Burdin, S.; Fairbairn, M.; Mermod, P.; Milstead, D.; Pinfold, J.; Sloan, T.; Taylor, W. Non-collider searches for stable massive particles. *Phys. Rept.* **2015**, *582*, 1–52. [CrossRef]
38. Jacobs, D.M.; Starkman, G.D.; Lynn, B.W. Macro Dark Matter. *Mon. Not. R. Astron. Soc.* **2015**, *450*, 3418–3430. [CrossRef]
39. Singh Sidhu, J.; Starkman, G.D. Reconsidering astrophysical constraints on macroscopic dark matter. *Phys. Rev. D* **2020**, *101*, 083503. [CrossRef]
40. Di Clemente, F.; Casolino, M.; Drago, A.; Lattanzi, M.; Ratti, C. Strange quark matter as dark matter: 40 years later, a reappraisal. *arXiv* **2024**, arXiv:2404.12094.
41. Di Clemente, F.; Drago, A.; Pagliara, G. Is the Compact Object Associated with HESS J1731-347 a Strange Quark Star? A Possible Astrophysical Scenario for Its Formation. *Astrophys. J.* **2024**, *967*, 159. [CrossRef]
42. Doroshenko, V.; Suleimanov, V.; Puehlhofer, G.; Santangelo, A. A strangely light neutron star within a supernova remnant. *Nat. Astron.* **2022**, *6*, 1444–1451. [CrossRef]
43. Suwa, Y.; Yoshida, T.; Shibata, M.; Umeda, H.; Takahashi, K. On the minimum mass of neutron stars. *Mon. Not. R. Astron. Soc.* **2018**, *481*, 3305–3312. [CrossRef]
44. Di Salvo, T.; Sanna, A.; Burderi, L.; Papitto, A.; Iaria, R.; Gambino, A.F.; Riggio, A. NuSTAR and XMM–Newton broad-band spectrum of SAX J1808.4–3658 during its latest outburst in 2015. *Mon. Not. R. Astron. Soc.* **2019**, *483*, 767–779. [CrossRef]
45. Perot, L.; Chamel, N.; Vallet, P. Unmasking strange dwarfs with gravitational-wave observations. *Phys. Rev. D* **2023**, *107*, 103004. [CrossRef]
46. Perot, L.; Chamel, N. Role of Quark Matter and Color Superconductivity in the Structure and Tidal Deformability of Strange Dwarfs. *Universe* **2023**, *9*, 382. [CrossRef]
47. Anglani, R.; Casalbuoni, R.; Ciminale, M.; Ippolito, N.; Gatto, R.; Mannarelli, M.; Ruggieri, M. Crystalline color superconductors. *Rev. Mod. Phys.* **2014**, *86*, 509–561. [CrossRef]
48. Kurban, A.; Huang, Y.F.; Geng, J.J.; Zong, H.S. Searching for Strange Quark Matter Objects Among White Dwarfs. *Phys. Lett. B* **2022**, *832*, 137204. [CrossRef]

49. Blouin, S.; Dufour, P.; Thibeault, C.; Allard, N.F. A New Generation of Cool White Dwarf Atmosphere Models. IV. Revisiting the Spectral Evolution of Cool White Dwarfs. *Astrophys. J.* **2019**, *878*, 63. [CrossRef]
50. Gaia Collaboration; Vallenari, A.; Brown, A.G.A.; Prusti, T.; de Bruijne, J.H.J.; Arenou, F.; Babusiaux, C.; Biermann, M.; Creevey, O.L.; Ducourant, C.; et al. Gaia Data Release 3—Summary of the content and survey properties. *Astron. Astrophys.* **2023**, *674*, A1. [CrossRef]